frontiers | Frontiers in Energy Research

TYPE Original Research
PUBLISHED 12 January 2023
DOI 10.3389/fenrg.2022.1044283

OPEN ACCESS

EDITED BY
Gianluigi De Falco,
DICMAPI—University of Naples Federico II, Italy

REVIEWED BY
Mingjiang Xie,
Huanggang Normal University, China
Pedro M. De Oliveira,
University of Cambridge,
United Kingdom

*CORRESPONDENCE
Jing Sun,
sunjing0108@163.com

SPECIALTY SECTION
This article was submitted to Process and Energy Systems Engineering, a section of the journal Frontiers in Energy Research

RECEIVED 14 September 2022
ACCEPTED 26 October 2022
PUBLISHED 12 January 2023

CITATION
Jia P, Sun J, Wang W, Song Z, Zhao X and Mao Y (2023), Study on the underpinning mechanisms of microwave-induced synthesis of carbon-coated metal nanoparticles. *Front. Energy Res.* 10:1044283. doi: 10.3389/fenrg.2022.1044283

Study on the underpinning mechanisms of microwave-induced synthesis of carbon-coated metal nanoparticles

Pingshan Jia, Jing Sun*, Wenlong Wang, Zhanlong Song, Xiqiang Zhao and Yanpeng Mao

National Engineering Laboratory for Reducing Emissions from Coal Combustion, Engineering Research Center of Environmental Thermal Technology of Ministry of Education, Shandong Key Laboratory of Energy Carbon Reduction and Resource Utilization, School of Energy and Power Engineering, Shandong University, Jinan, China

Microwave-induced metal arc discharge provides an intriguing solution for the synthesis of carbon-coated metal nanoparticles (M@CNPs) due to its fast formation and improved quality of products, however, the underpinning reaction mechanism is not comprehensively revealed. In this work, the effect of arc discharge intensity on the product morphology is firstly investigated by adjusting microwave power. And then, the effects of the organic groups (i.e. cyclopentadienyl v. s Acetylacetonate groups) and metal catalysis on the product morphology are also investigated by selecting ferrocene, iron acetylacetonate, nickelocene, and nickel acetylacetonate as precursors. Specifically, moderate microwave power can not only destroy the precursor to form carbon nanosheets by inducing intense discharge heat release but also provide sufficient intermittency to allow the carbon nanosheets to deposit on the surface of the metal core, which is an important precondition in fabricating M@CNPs. The structure of organic groups in the precursor also plays a predominant role in adjusting product morphology. Cyclopentadienyl groups tend to encapsulate the metal core to form graphitized carbon shells as the coordination bond between cyclopentadienyl and metal is recognized as a very strong covalent bond that confines the cyclopentadienyl collapse to metal core, and the cyclic structure facilitates the formation of graphite. In contrast, the acetylacetonate groups intend to combine randomly due to their open-loop structure. Moreover, for open-loop structures such as acetylacetonate groups, metal catalysis also affects the growth trend, of which Ni is more likely to induce the formation of carbon nanotubes relative to Fe. This work can provide a good reference for the synthesis of M@CNPs with controllable morphology.

KEYWORDS

microwave, carbon-coated metal nanoparticles, growth mechanism, arc discharge, nanotube

1 Introduction

Metal/carbon nanocomposite materials have attracted tremendous interest from researchers thanks to their strong potential for optical and electronic devices, energy storage, catalysis, and other novel applications (Yan et al., 2017; Ohtaka, 2019; Gao et al., 2021). As a special kind of composite material with a core-shell structure, carbon-coated metal nanoparticles (M@CNPs) have been one of the most potential nanomaterials due to technological importance stemming from their novel properties that are different from bulk materials and bare metal NPs (Zhou et al., 2009; Liu et al., 2020). For M@CNPs, the carbon shell can not only protect the metal core against oxidization and agglomeration to form bigger crystallites (Byeon and Kim, 2010), but also can endow these nanoparticles with further function (Wu et al., 2012), resulting in important applications in energy storage (Wu et al., 2020), catalysis (Park et al., 2019), magnetic carrier (Ayguen et al., 2018), and drug delivery (Zhong et al., 2022). Owing to the excellent performance and wide applications, many efforts have been dedicated to the synthesis of M@CNPs, including physical vapor deposition (PVD) (Dai and Moon, 2018) such as arc discharge, chemical vapor deposition (CVD) (Gallego et al., 2011), pyrolysis of carbon materials (Geng et al., 2007), hydrothermal reaction (Cao et al., 2012), and wet-chemical route (Wang et al., 2006). However, some of these methods are energy-consuming or time-consuming, while others require the assistance of specialized equipment, which will become an obstacle to large-scale practical application (Ahsan et al., 2021). Therefore, a green and sustainable technique to form these composites is urgently needed.

As an intriguing solution, our recent study found that microwave-induced metal arc discharge can be adopted as a new pathway to synthesize high-purity carbon-coated iron nanoparticles (Fe@CNPs) by using ferrocene as the precursor, nonpolar organic hydrocarbons (benzene and cyclohexane) as solvents and tungsten wires as the initiator to induce microwave-metal discharges therein (Sun et al., 2017; Wang et al., 2018). This is mainly attributed to the microwave-induced metal arc discharge process being pulsed rather than continuous, providing fundamentally pulsed thermal shock which can promote the decomposition of precursors and graphitization of organic groups by the instant release of intense discharge heat, whilst limiting the growth of nanotube owing to the absent of energy supply in the discharge gap and the fast quenching by the surrounding media. Owing to this featured arc discharge, this liquid-phase synthetic method enables a high yield of high-purity Fe@CNPs with the merits of high efficiency, simplicity, excellent core-shell structures, and well graphitization of the carbon shell. More importantly, the synthesis process is milder than the conventional high-temperature graphitization method (i.e. CVD), since microwave-induced metal arc discharge can be initiated easily in a low-power microwave oven. The enhancement of Fe@CNPs yield and quality by using our featured microwave-metal discharge-driven reactions is intriguing, however, the underpinning growth mechanism, regardless of the synthesis method, has not been comprehensively revealed.

Although the pulsed heating effect of discharges contributes to the synthesis of high-purity Fe@CNPs, the *in-situ* catalysis of iron and the structure of precursor's organic groups (carbon sources) may be other contributing factors. In literature, transition metals represented by Fe, Ni and Co. are widely recognized on catalyzing carbonization of carbon precursors to form highly graphitized carbon nanostructure (Ruemmeli et al., 2011; Li et al., 2014; Hunter et al., 2022). Moreover, whether the cyclopentadienyl group of ferrocene contributes to shell graphitization is still unclear. Whether this featured synthesis method can be extended to synthesize Fe@CNPs by using other organometallic compounds (such as iron acetylacetonate) or other similar metal nanoparticles (such as Co.@CNPs and Ni@CNPs) by using other corresponding organic precursor are also still unknown. Furthermore, the influencing factors may affect the growth process in a coupled way rather than individually, leading to the difficulty in revealing the underpinning mechanisms. Therefore, comprehensive investigations should be conducted to reveal the underpinning mechanisms.

In this paper, carbon-coated metal nanoparticles (M@CNPs) were synthesized by microwave-induced metal arc discharge to investigate the formation mechanism during the reaction and the influencing factors of the product morphology. Ferrocene, iron acetylacetonate, nickelocene, and nickel acetylacetonate were selected as the precursors for carbon and metal sources to explore the effects of arc discharge intensity and precursors on product morphology, respectively. The structural characteristics of products were comprehensively analyzed by means of SEM and TEM. This work is devoted to the comprehensive study and discussion on the formation mechanism of M@CNPs synthesized by microwave-induced arc discharge and provides a reference for the controllable and efficient preparation of M@CNPs.

2 Methodology

2.1 Materials

In this typical experiment, ferrocene ($FeC_{10}H_{10}$), nickelocene ($NiC_{10}H_{10}$), iron acetylacetonate ($C_{15}H_{21}FeO_6$), and nickel acetylacetonate ($C_{10}H_{14}NiO_4$) were acted as precursors, cyclohexane and benzene were selected as the organic solvents, all of them were purchased from Aladdin Industrial Corporation. Tungsten wires (Φ0.5 mm, 6 mm long) were used to induce metal arc discharge in a customized industrial microwave oven (100–1500 W, 2.45 GHz). Ethanol and

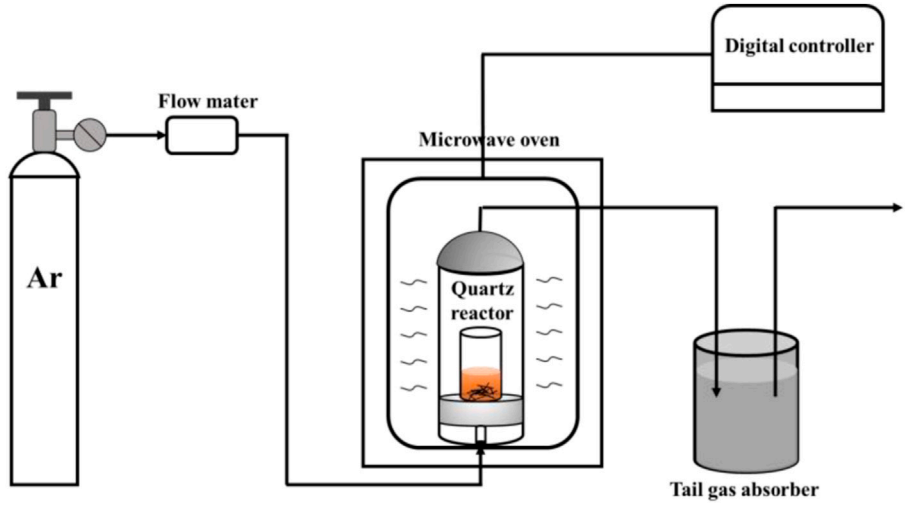

FIGURE 1
Schematic diagram of experimental device.

concentrated nitric acid purchased from Sinopharm Chemical Reagent Co. Ltd. were used for the purification of products, mainly for removing unreacted materials and amorphous carbon. Incidentally, the concentrated nitric acid was diluted to 3 mol L^{-1} by deionized water. High purity argon (99.999%) obtained from Jinan De Yang Special Gases Co. Ltd. served as a protective gas. A wave-transparent, high-temperature resistant, custom-designed quartz reactor was used for the synthesis of carbon-coated metal nanoparticles based on microwave-induced metal arc discharge.

2.2 Sample preparation

As shown in Figure 1, in each experiment, the organic solvent and precursor were first mixed with a weight ratio of 15:1 in a small quartz tube (inner Φ30 mm, 50 mm high), in which were 0.6 g precursor (i.e. ferrocene, nickelocene, iron acetylacetonate, and nickel acetylacetonate) dispersed in 9 g solvent (cyclohexane/benzene). Considering the difference in solubility, cyclohexane was selected as the solvent for ferrocene and iron acetylacetonate while nickelocene and nickel acetylacetonate were dissolved in benzene, ensuring the full dissolution of precursor in organic solvent. After that, the mixture was hermetically heated in a water bath at the temperature of 80 °C for 10 min and then the tungsten wires (2 g) were added to the mixture. Then, every quartz tube containing the mixture was placed in the customized quartz reactor and then in the industrial microwave oven. To ensure an oxygen-free condition during the reaction, argon gas was introduced at 200 ml min^{-1} to purge the air inside before starting the microwave radiation. In order to investigate the underpinning mechanism of the synthesis of carbon-coated metal nanoparticles in the microwave power range of 500-1500 w, 3-min radiation was selected as the typical reaction time according to repeated experiments, because the reaction is not completed if the reaction time is too short, while long reaction time promotes the formation of carbon nanotubes which will conceal the formation mechanism of carbon-coated nanoparticles. Therefore, the mixture was exposed to microwave radiation with discharge phenomenon for 3 min at a power ranging from 500 to 1500 W with an Ar flow rate of 200 ml min^{-1}. During microwave irradiation, a violent discharge phenomenon can be seen at the tips of the tungsten wire, and the quartz tube gradually turned black as the reaction progresses. After the reaction, the reactor was naturally cooled down to ambient temperature in an argon atmosphere. The M@CNPs were collected from the reactor and were washed for 3 h with dilute nitric acid (3 M) to remove the residual precursor and incomplete coated metal nanoparticles. Immediately, the solid product was washed three times with ethanol and deionized water to remove the amorphous carbon. The remaining products were then dried for 6 h at 80 °C to obtain the purified products.

2.3 Characterization

Scanning electron microscope (SEM, SUPRA™55, ZEISS, Germany) was used to characterize the morphology of as-prepared samples. And the microstructure of the samples dispersed in a standard copper mesh after ultrasonic dispersion in ethanol solvent was analyzed in detail by transmission electron microscopy (TEM, FEI).

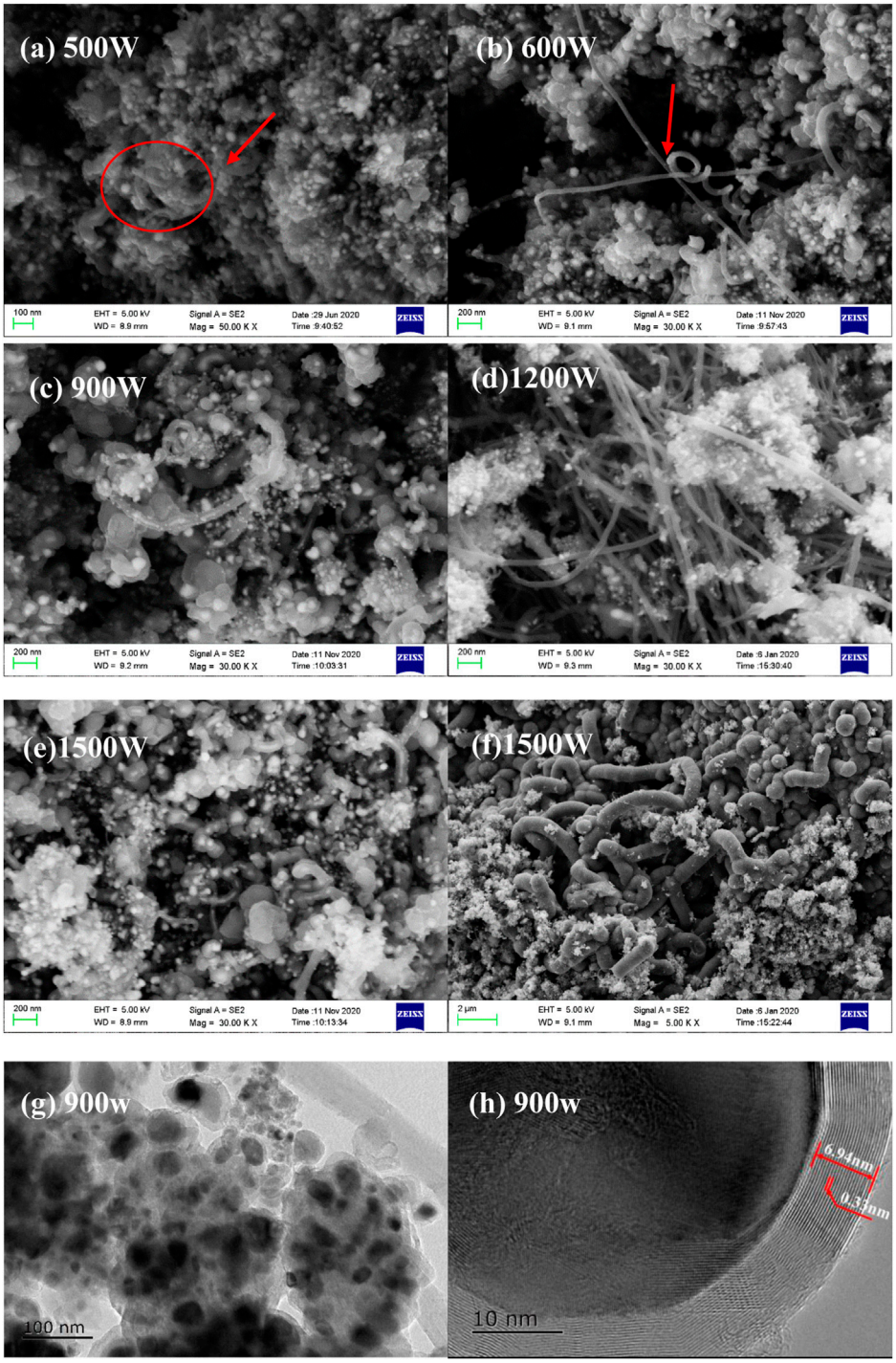

FIGURE 2
SEM of the products derived from ferrocene dissolved in cyclohexane at different microwave power **(A–F)**; TEM of products derived at a microwave power of 900 W **(G,H)**.

3 Results and discussions

3.1 The effect of discharge intensity

Under microwave irradiation, tungsten wire induces intense arc discharge, which instantly produces a high-temperature environment and promotes the decomposition of organometallic compound (Zhan et al., 2017). Since the discharge intensity and frequency is proportional to the microwave power when otherwise conditions are unchanged Sun et al., 2021; Gao et al., 2020, the effect of microwave power on the product morphology was firstly overviewed by using 9 g cyclohexane as the organic solvent, 0.6 g ferrocene as the metal source, and 2 g Tungsten wires as the discharge triggering media. As shown in Figure 2, due to the strong thermal shock caused by arc discharge, ferrocene is transformed into Fe/carbon nanocomposites, and the morphology changes significantly with microwave power. As shown in Figures 2A,B, the products synthesized at the microwave power of 500W and 600 W are mainly nanoparticles, with few amount of nanotubes present. When the microwave power is increased to 900 W, the nanoparticles tend to grow owing to agglomeration, and form some metal filled nanotubes as pointed by the red arrow. With the further increase of microwave power, the Fe particles tend to reduce in size and agglomerate, meanwhile, nanotubes are massively generated, as illustrated in Figures 2D,F. It can be inferred that lower power (<900 W) is conducive to synthesizing the carbon encapsulated iron particles, while high power promotes the formation of carbon nanotubes. As ferrocene cannot be efficiently heated by microwave, sublimes significantly at 100 °C, and can be thermal stable at a temperature up to 470°C, the formation of carbonaceous product can be inferred as instant thermal shock induced by arc discharge.

With regard to the effect of microwave power on the product morphology, it is in essence the effect of discharge intensity. As the metal wires are exposed to a microwave field, a strong electric field can be formed on their tips, inducing an increase in the electron density to initiate the electron breakdown avalanche. Owing to the field enhancement, the ohmic heating of the conductive electrons are also strengthened, allowing for more electrons in the initiator tip can occupy states above the Fermi level and possess a higher tunneling probability. When electrons are emitted from the initiator tip, the initial seed electrons multiply under the influence of the supercritical electric field, leading to stronger ionization with the formation of energetic electrons, ions, and reactive radicals. From that point, the formation of a plasma filament or so-called discharge occurs, with the release of heat as a result of Joule heating of the partial or full breakdown current and photons as a result of activated electrons transitioning back to their ground state. Subsequently, the effective electron collision frequency decreases to a low level several microseconds after the discharge, meaning that the discharge cycle has finished (Sun et al., 2021). And then, another discharge circle repeats the same procedure. Definitely, the higher input microwave power means higher electric field to initiate the electron breakdown, and thereby, enhance the discharge intensity and frequency (Gao et al., 2020). Therefore, at lower microwave power, a pulsed discharge thermal shock causes the decomposition and carbonization of organic groups, while the discharge intermittency allows the carbon nanosheet to deposit on the metal nanoparticles to form carbon shells. In contrast, under high microwave power, intense discharge heat release with shortened intermittency does not allow the carbon nanosheets to be evenly deposited on the metal surface but promotes them to recombine and grow into carbon nanotubes under the high temperature, leading to the generation of nanotubes (Bai et al., 2003; Huang and Weng, 2011). Therefore, pulsed thermal shock with considerable intermittent is thereby favorable for the formation of Fe@CNPs whilst limiting the growth of nanotubes.

The TEM result shown in Figure 2G indicates that carbon-coated iron nanoparticles with an obvious core-shell structure were formed. The iron cores wrapped in the carbon shell have different sizes and present certain agglomeration which is mainly due to the strong cohesion and electromagnetic effect of iron nanoparticles. As shown in Figure 2H, the iron core is covered with a highly crystalline carbon shell with a thickness of about 6.94 nm. The carbon shell presents a high degree of graphitization as the carbon shell had good integrity with a layer spacing of about 0.33 nm, which is very similar to the theoretical crystal spacing (0.3354 nm) of graphite layers (Lu et al., 2005). The formation mechanisms were speculated as: although neither nonpolar solvent nor ferrocene can be effectively heated by microwave, the thermal effect caused by the arc discharge triggered by tungsten wire can instantly create a high temperature to promote the decomposition or chemical bond cleavage of ferrocene. As the coordination bond between cyclopentadienyl and metal is recognized as a very strong covalent bond whose thermal dissociation energy even exceeds the bond energy of carbon-carbon single bond (Sha et al., 2018), the collapse of cyclopentadienyl groups by discharge thermal shock are mostly confined to the metal cores and deposit on their surface during the two consecutive discharge gaps, promoting the formation of core-shell structure. With the increase of temperature, the organic layer on the core surface gets pre-carbonization, forming as a dielectric material with enhanced microwave absorption to further accelerate the carbonization (Liang et al., 2018; Bo et al., 2019; Tumuluru et al., 2021). As the structure of ferrocene is an iron atom between two parallel cyclopentadienyl groups and the pentagon ring can induce the formation of Stone-Wales graphene (Xie et al., 2018), the ring structure of cyclopentadienyl is favorable for the formation of graphite, which is highly consistent with TEM results. Furthermore, as is widely proved, the iron core can catalyze

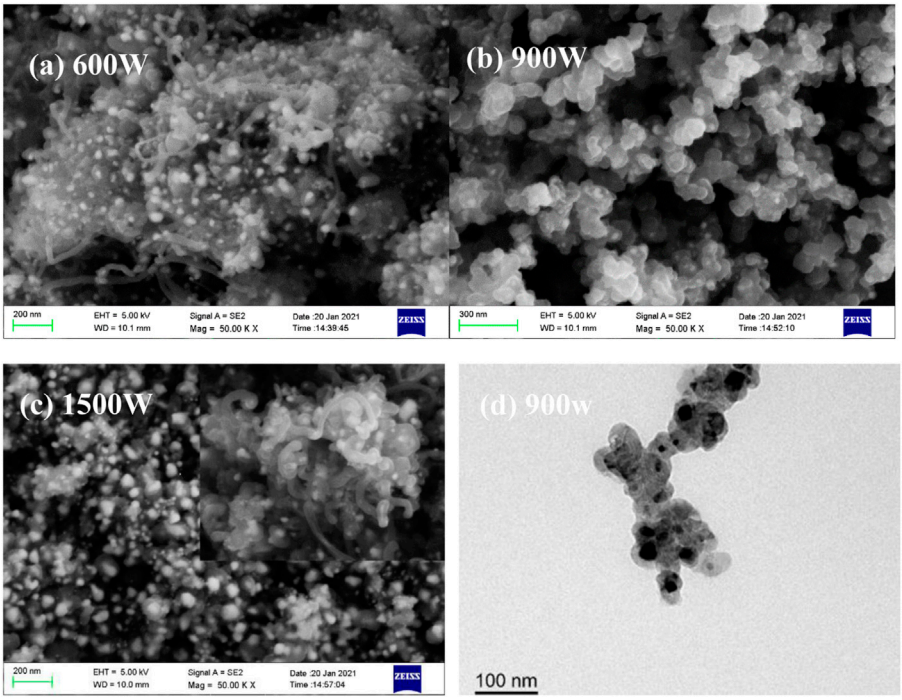

FIGURE 3
SEM **(A–C)** images of the products derived from nickelocene dissolved in benzene at different power and TEM **(D)** of the products derived at a microwave power of 900 W.

the carbon shell graphitization, finally leading to the formation of Fe@CNPs with well-graphitized shells (Sun et al., 2022). Conclusively, both the ring structure of the cyclopentadienyl group and the catalytic effect of iron may contribute to the formation of a graphitized carbon shell. The existence of iron-filled carbon nanotubes further indicates that under intense discharge, the catalysis of the iron core can promote the growth and extension of carbon nanosheets (Lee et al., 2004). Therefore, the morphology of the products under various discharge intensities reveals that the control of microwave power plays an important role in adjusting the products towards nanoparticles or nanotubes.

Microwave power also plays an important role in the product nanostructures when nickelocene is used as the precursor. As shown in Figure 3, carbon-coated Ni nanoparticles (Ni@CNPs) are formed by metal discharge, however, a considerable amount of nanotubes are generated both in the lower (600 W) and higher (1500 W) microwave power. According to the above speculation, a large number of nanotubes are produced at high power (1500 W) mainly due to the catalytic growth of carbon nanosheet in the high-temperature environment induced by high-frequency discharge with shortened discharge intermittency. As for the nanotubes present in products at 600W, it may be caused by the synergy effect of local overheating as a result of uneven discharges and Ni catalysis or the low discharge heat release and relatively long intermittency facilitate the Ni-catalytic growth of cyclopentadienyl groups to form nanotubes (Zhang et al., 2011), which worth in-depth investigation in future. Importantly, it is interesting to note that relatively uniform and purified Ni@CNPs (Figure 3B) with core-shell structures (Figure 3D) were generated at a microwave power of 900W, confirming the speculation that moderate discharge intermittency is conducive to the deposition of carbon fragments to form Ni@CNPs.

In general, the discharge intensity has an important influence on the morphology of products, especially in determining the growth of nanoparticles. On the one hand, arc discharge provides sufficient energy for the formation of products. Both ferrocene and nickelocene, as precursors, need sufficient energy to realize the destruction of chemical bonds and carbonization. And then, the aggregation of metal atoms and deposition of carbon precursors are completed during the discharge intermittency. On the other hand, the intensity of arc discharge has a significant effect on the growing trend of products. Although microwave-induced arc discharge has pulse property, the high-intensity discharge will greatly improve the reaction temperature, which is conducive to the formation of metal-catalyzed carbon nanotubes. Therefore, reasonable control of microwave power, that is, control of discharge intensity, will make it possible for the

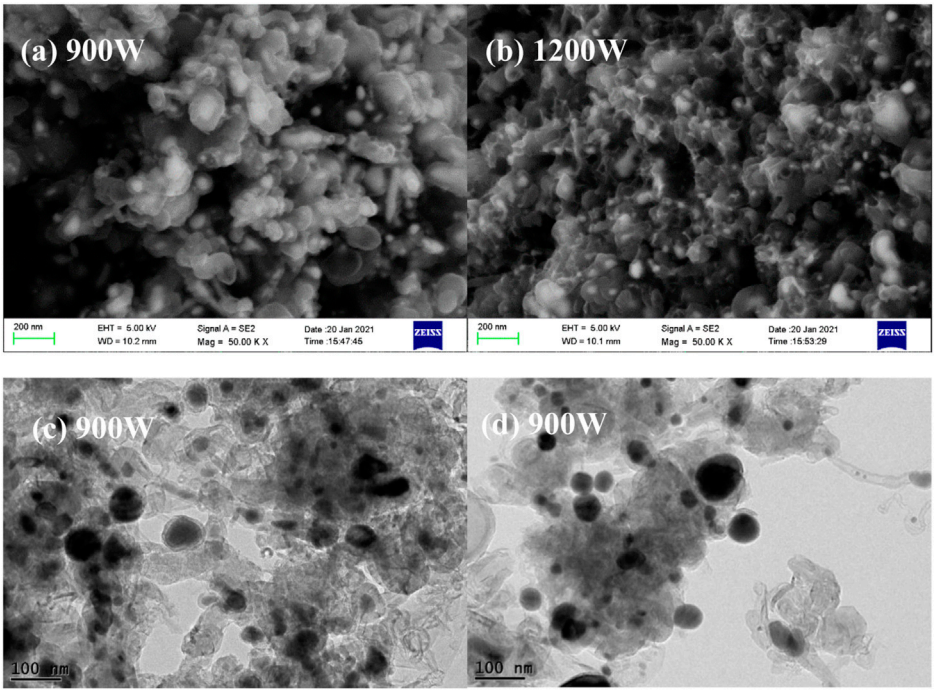

FIGURE 4
SEM **(A,B)** of the products derived from iron acetylacetonate dissolved in cyclohexane at different power and TEM **(C,D)** of the products at 900 W.

regulated products to grow in different morphology (nanoparticles or nanotubes).

3.2 The effect of precursors

In addition to microwave power, different precursors may have potential effects on the products of arc discharge. Specifically, the structure of organic groups in the precursor may affect the morphology of carbonized products, and the metal atoms of the precursor may play a potential catalytic role, leading to different growth trends of products. Hence, the effects of different precursors on the structure and morphology of products will be discussed to further explain the mechanism during the products' growth. Based on our above inference, the products obtained from iron acetylacetonate and nickel acetylacetonate were further investigated and compared with the two precursors mentioned above to confirm the effects of organic groups on the growth mechanism.

When the precursor is changed into iron acetylacetonate, the discharge intensity also has a significant effect on the morphology products. As shown in Figure 4A, at a microwave power of 900W, the products present an obvious carbon-coated nanoparticle structure, with a few short metal-filled carbon nanotubes attached. Furthermore, the obtained carbon-coated nanoparticles present agglomeration, leading to the formation of relatively large particles. Further analysis on the structure of the products at the power of 900 W are carried out by TEM. As shown in Figures 4C,D, in addition to the nanoparticles with core-shell structure observed in SEM, there are a small number of uncoated particles and hollow carbon shells in the spherical particles, which may be attributed to the fact that carbon nanosheets formed by carbonization of acetylacetonate groups are not completely deposited on the surface of iron particles or the carbon shell is not intact. Moreover, metal filled carbon nanotubes also appear in the products, which are characterized by the outward extension of the carbon layer with the core of metal particles. When the microwave power is increased to 1200W, spherical particles tend to reduce in size and the carbon layers on the surface of some particles are bridged together as shown in Figure 4B, indicating the carbon nanosheets formed by carbonization of acetylacetonate groups grow randomly at high temperature.

Compared with cyclopentadienyl structure, the iron acetylacetonate investigated herein are coordination complexes characterized by center metal ions bridged with acetylacetonate anion. Therefore, besides atomic iron, the pyrolysis of iron acetylacetonate at high temperature will obtain the

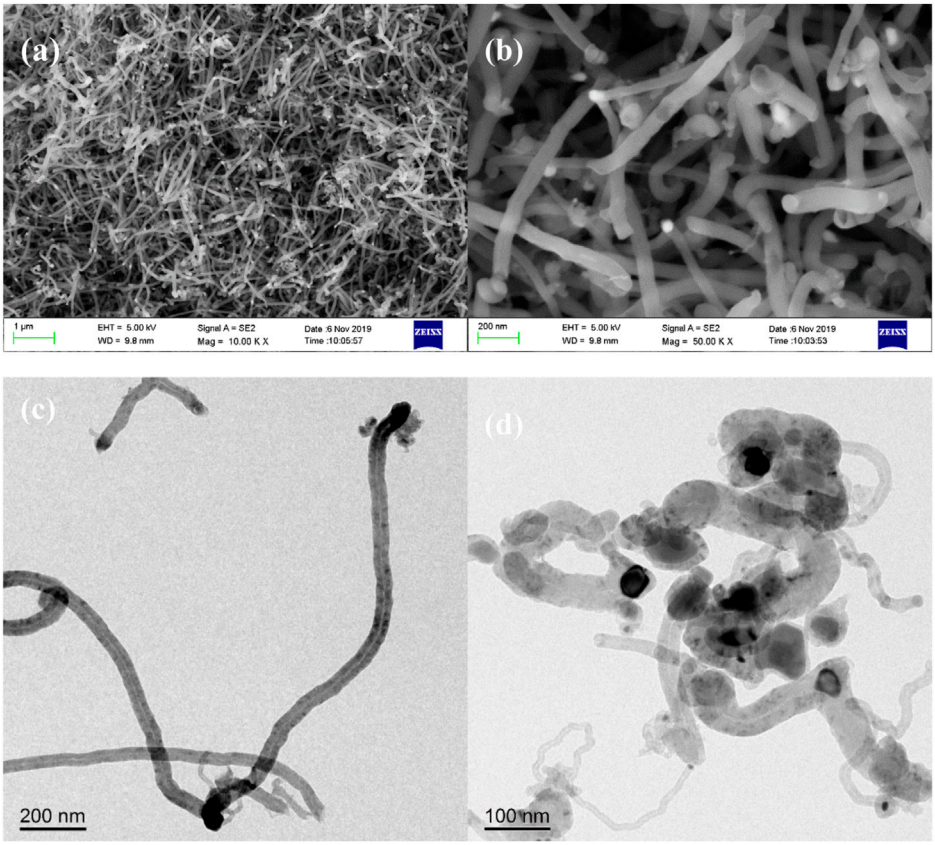

FIGURE 5
SEM **(A,B)** and TEM **(C,D)** images of the products derived from nickel acetylacetonate dissolved in benzene at 900 W.

acetylacetonate group which is an open-loop structure different from the cyclopentadienyl group. Both of the iron cores derived from ferrocene and iron acetylacetonate present an agglomeration phenomenon, indicating that iron atoms tend to aggregate into nanoparticles after separation from organic groups. Unlike the products derived from ferrocene, uncoated and incompletely coated particles and even hollow carbon shells all increase in amount in the products derived from iron acetyacetonate, indicating that the open-loop structure of organic groups facilitates the random growth of carbon nanosheets rather than confine them to the surface of metal cores.

The morphology difference between these two products indicates that the organic group has a significant effect on the growth of the product. The cyclopentadienyl group released by ferrocene is structurally different from the acetylacetonate group from iron acetylacetonate. Based on stronger chemical stability, the cyclopentadienyl groups tend to deposit on the surface of the iron core. And then, it carbonizes to form a common core-shell structure with the catalysis of metallic iron. A small number of nanotubes in the products (Figure 2) are mainly due to the promotion of continuous high temperature on the formation of nanotubes. For acetylacetonate groups, the open-loop structure makes them more inclined to combine freely under the catalysis (Arod and Shivashankar, 2015), rather than being bound to the metal surface, so there are more hollow carbon shells and incompletely coated metal particles due to the free combination of organic groups in the products.

In order to further verify the influence of organic groups on the morphology of products, the products of nickelocene and nickel acetylacetonate were compared. For the products of nickelocene, both Ni@CNPs and nanotubes can be found in the products, but the yield of Ni@CNPs will be greatly increased by controlling the power to set the appropriate discharge intensity and frequency, which further suggests that cyclopentadienyl groups are more conducive to the formation of core-shell structure. Combined with the morphology of Fe@CNPs derived from ferrocene, it can be speculated that

cyclopentadienyl groups with the cyclic structure are more inclined to deposit on the surface of metal nanoparticles and carbonize to form shells, to construct M@CNPs with core-shell structure.

In contrast, as shown in Figures 5A,B, the products are nanotubes with almost no nanoparticles when the precursor changed into nickel acetylacetonate, in which the nanotubes with the shape that metal core filled as the end point can be observed. Figures 5C,D show the TEM of the products derived from nickel acetylacetonate. Obviously, the metal cores appear in the nanotube, and the carbon shell will extend outward along the metal core, triggering the formation of metal filled at the end or the center of nanotubes, which indicates that the formation of the nanotubes may rely on the catalysis of the metal core (Yao et al., 2020). Moreover, the nanotubes in Figure 5 are very uniform in diameter and grows in a certain length range, which indicates that the acetylacetonate group is more inclined to form nanotube structure and the extension of structure relies on the catalysis of metal cores. These significant differences obviously come from the structure of organic groups.

It can be concluded that the structure of the organic group has an important influence on the morphology of the product. According to the previous conclusion, under the high-temperature conditions created by arc discharge, the chemical bond between metal atoms and carbon precursors will be destroyed, resulting in separation. In the subsequent reaction stage, the free metal atoms tend to aggregate into the metal core, and the free carbon precursor will form different morphologies due to the influence of structure. Cyclopentadienyl groups are more inclined to deposit on the surface of the metal core to form graphitized carbon, which forms carbon-coated metal nanoparticles (M@CNPs) with a core-shell structure. As for acetylacetonate groups, accompanied by the breaking of the chemical bond with the metal atom, the free groups are easier to combine freely under the catalysis and cannot completely cover the surface of the metal core, which explains the formation of more nanotubes and hollow carbon shells.

In addition, different metal atoms will affect the growth trend of the same carbon source groups. For cyclopentadienyl groups with more stable structures, the products are mainly nanoparticles with core-shell structure at a moderate microwave power. However, it is worth noting that under the same microwave power of 600W, the yield of nanotubes in products of nickelocene products is significantly higher than those in ferrocene products, implying that metal catalysis also affect the growth trends of products. When the precursor is changed to the acetylacetonate group with a open-loop structure, the morphology of products also shows great differences, in which uniform nanotube structure is formed for nickel acetylacetonate, while the product of iron acetylacetonate is the coexistence of particles and nanotubes. Therefore, the type of metal also has an important influence on the growth trend of nanoparticles. It is inferred that Ni is more inclined to promote the formation of nanotubes compared with Fe.

4 Conclusion

In summary, microwave-induced tungsten arc discharge is a potential method to produce carbon-coated metal nanoparticles (M@CNPs). To explore the effects of arc discharge intensity and precursors on the morphology of M@CNPs, ferrocene, iron acetylacetonate, nickelocene, and nickel acetylacetonate were selected as carbon and metal sources. Firstly, microwave power has a significant effect on controlling the growth trends of the products. Arc discharge provides energy for the decomposition of precursors and promotes the aggregation of metal atoms and the carbonization of organic groups, while the discharge intermittency will make it possible to deposit carbon nanosheets on the metal core surface. In this case, moderate power is conducive to the generation of core-shell structure, while higher power promotes the formation of nanotubes. And then, organic groups of precursors have significant effects on the morphology. Specifically, cyclopentadienyl group, as a cyclic structure, tends to deposit on the metal surface to form a highly graphitized carbon coated core-shell structure, while acetylacetonate groups with open-loop structure tend to combine freely and cannot completely cover the metal cores, resulting in the formation of hollow carbon shells and carbon nanotubes. Moreover, the metal core has significant directional catalysis on some organic groups. Especially for open-loop structures such as acetylacetonate groups, Ni is more inclined to promote the formation of nanotubes relative to Fe. In conclusion, based on the above research, the required Metal/Carbon composites can be efficiently synthesized by adjusting the microwave power to match the discharge intensity with the intermittency, and selecting the precursor to match the metal type with the organic group. Importantly, this work not only provides a method for the preparation of carbon-coated metal nanoparticles or metal-filled nanotubes but also provides insights into the synthesis of Metal/Carbon composites with directionally controlled morphology.

Data availability statement

The original contributions presented in the study are included in the article/supplementary material, further inquiries can be directed to the corresponding author.

Author contributions

PJ: Conceptualization, Investigation, Data Curation, Experimental analysis, Writing—Original Draft JS:

Writing—Review and Editing, Validation, Methodology, Funding acquisition WW: Supervision, Validation, Conceptualization ZS: Project administration, Supervision XZ: Validation, Formal analysis YM: Resources, Validation.

Funding

This work was generously supported by the Natural Science Foundation of Shandong Province (ZR2019MEE035) and the Young Scholars Program of Shandong University (2018WLJH75).

Conflict of interest

The authors declare that the research was conducted in the absence of any commercial or financial relationships that could be construed as a potential conflict of interest.

Publisher's note

References

Ahsan, M. A., Puente Santiago, A. R., Sanad, M. F., Mark Weller, J., Fernandez-Delgado, O., Barrera, L. A., et al. (2021). Tissue paper-derived porous carbon encapsulated transition metal nanoparticles as advanced non-precious catalysts: Carbon-shell influence on the electrocatalytic behaviour. *J. Colloid Interface Sci.* 581, 905–918. doi:10.1016/j.jcis.2020.08.012

Arod, P., and Shivashankar, S. A. (2015). Single-step synthesis of carbon nanotubes/iron/iron oxide composite films through inert-ambient CVD using ferric acetylacetonate as a precursor. *RSC Adv.* 5, 59463–59471. doi:10.1039/c5ra07472j

Ayguen, M., Chamberlain, T. W., Gimenez-Lopez, M. d. C., and Khlobystov, A. N. (2018). Magnetically recyclable catalytic carbon nanoreactors. *Adv. Funct. Mat.* 28, 1802869. doi:10.1002/adfm.201802869

Bai, S., Li, F., Yang, Q. H., Cheng, H. M., and Bai, J. (2003). Influence of ferrocene/benzene mole ratio on the synthesis of carbon nanostructures. *Chem. Phys. Lett.* 376, 83–89. doi:10.1016/s0009-2614(03)00959-x

Bo, X., Xiang, K., Zhang, Y., Shen, Y., Chen, S., Wang, Y., et al. (2019). Microwave-assisted conversion of biomass wastes to pseudocapacitive mesoporous carbon for high-performance supercapacitor. *J. Energy Chem.* 39, 1–7. doi:10.1016/j.jechem.2019.01.006

Byeon, J. H., and Kim, J.-W. (2010). Morphology and structure of aerosol carbon-encapsulated metal nanoparticles from various ambient metal-carbon spark discharges. *ACS Appl. Mat. Interfaces* 2, 947–951. doi:10.1021/am100015a

Cao, C., Ma, Z., Ma, C., Pan, W., Liu, Q., and Wang, J. (2012). Synthesis and characterization of Fe/C core-shell nanoparticles. *Mat. Lett.* 88, 61–64. doi:10.1016/j.matlet.2012.08.041

Dai, W., and Moon, M. W. (2018). Carbon-encapsulated metal nanoparticles deposited by plasma enhanced magnetron sputtering. *Vacuum* 150, 124–128. doi:10.1016/j.vacuum.2018.01.037

Gallego, J., Sierra, G., Mondragon, F., Barrault, J., and Batiot-Dupeyrat, C. (2011). Synthesis of MWCNTs and hydrogen from ethanol catalytic decomposition over a Ni/La2O3 catalyst produced by the reduction of LaNiO3. *Appl. Catal. A General* 397, 73–81. doi:10.1016/j.apcata.2011.02.017

Gao, C., Lyu, F., and Yin, Y. (2021). Encapsulated metal nanoparticles for catalysis. *Chem. Rev.* 121, 834–881. doi:10.1021/acs.chemrev.0c00237

Gao, Y., Mao, Y., Song, Z., Zhao, X., Sun, J., Wang, W., et al. (2020). Efficient generation of hydrogen by two-step thermochemical cycles: Successive thermal reduction and water splitting reactions using equal-power microwave irradiation and a high entropy material. *Appl. Energy* 279. doi:10.1016/j.apenergy.2020.115777

Geng, J., Jefferson, D. A., and Johnson, B. F. G. (2007). The unusual nanostructure of nickel-boron catalyst. *Chem. Commun.*, 969–971. doi:10.1039/b615529d

Huang, G., and Weng, J. (2011). Syntheses of carbon nanomaterials by ferrocene. *Curr. Org. Chem.* 15, 3653–3666. doi:10.2174/138527211797884593

Hunter, R. D., Ramirez-Rico, J., and Schnepp, Z. (2022). Iron-catalyzed graphitization for the synthesis of nanostructured graphitic carbons. *J. Mat. Chem. A Mat.* 10, 4489–4516. doi:10.1039/d1ta09654k

Lee, D. C., Mikulec, F. V., and Korgel, B. A. (2004). Carbon nanotube synthesis in supercritical toluene. *J. Am. Chem. Soc.* 126, 4951–4957. doi:10.1021/ja031522s

Li, Q., Cao, R., Cho, J., and Wu, G. (2014). Nanocarbon electrocatalysts for oxygen reduction in alkaline media for advanced energy conversion and storage. *Adv. Energy Mat.* 4, 1301415. doi:10.1002/aenm.201301415

Liang, J., Qu, T., Kun, X., Zhang, Y., Chen, S., Cao, Y.-C., et al. (2018). Microwave assisted synthesis of camellia oleifera shell-derived porous carbon with rich oxygen functionalities and superior supercapacitor performance. *Appl. Surf. Sci.* 436, 934–940. doi:10.1016/j.apsusc.2017.12.142

Liu, J., Xie, L., Wang, Z., Mao, S., Gong, Y., and Wang, Y. (2020). Biomass-derived ordered mesoporous carbon nano-ellipsoid encapsulated metal nanoparticles inside: Ideal nanoreactors for shape-selective catalysis. *Chem. Commun.* 56, 229–232. doi:10.1039/c9cc08066j

Lu, Y., Zhu, Z. P., and Liu, Z. Y. (2005). Carbon-encapsulated Fe nanoparticles from detonation-induced pyrolysis of ferrocene. *Carbon* 43, 369–374. doi:10.1016/j.carbon.2004.09.020

Ohtaka, A. (2019). Transition-metal nanoparticles catalyzed carbon-carbon coupling reactions in water. *Curr. Org. Chem.* 23, 689–703. doi:10.2174/1385272823666190419211714

Park, H.-S., Han, S.-B., Kwak, D.-H., Han, J.-H., and Park, K.-W. (2019). Fe nanoparticles encapsulated in doped graphitic shells as high-performance and stable catalysts for oxygen reduction reaction in an acid medium. *J. Catal.* 370, 130–137. doi:10.1016/j.jcat.2018.12.015

Ruemmeli, M. H., Bachmatiuk, A., Boerrnert, F., Schaeffel, F., Ibrahim, I., Cendrowski, K., et al. (2011). Synthesis of carbon nanotubes with and without catalyst particles. *Nanoscale Res. Lett.* 6, 303. doi:10.1186/1556-276x-6-303

Sha, Y., Zhang, Y., Xu, E., Wang, Z., Zhu, T., Craig, S. L., et al. (2018). Quantitative and mechanistic mechanochemistry in ferrocene dissociation. *ACS Macro Lett.* 7, 1174–1179. doi:10.1021/acsmacrolett.8b00625

Sun, J., Wang, Q., Wang, W., Song, Z., Zhao, X., Mao, Y., et al. (2017). Novel treatment of a biomass tar model compound via microwave-metal discharges. *Fuel* 207, 121–125. doi:10.1016/j.fuel.2017.06.075

Sun, J., Yu, G., An, K., Wang, W., Wang, B., Jiang, Z., et al. (2021). Microwave-induced high-energy sites and targeted energy transition promising for efficient energy deployment. *Front. Energy*. doi:10.1007/s11708-021-0771-y

Sun, Z., Yao, D., Cao, C., Zhang, Z., Zhang, L., Zhu, H., et al. (2022). Preparation and formation mechanism of biomass-based graphite carbon catalyzed by iron nitrate under a low-temperature condition. *J. Environ. Manag.* 318, 115555. doi:10.1016/j.jenvman.2022.115555

Tumuluru, J. S., Ghiasi, B., Soelberg, N. R., and Sokhansanj, S. (2021). Biomass torrefaction process, product properties, reactor types, and moving bed reactor design concepts. *Front. Energy Res.* 9. doi:10.3389/fenrg.2021.728140

Wang, Y., Wang, W., Sun, J., Sun, C., Feng, Y., and Li, Z. (2018). Microwave-based preparation and characterization of Fe-cored carbon nanocapsules with novel stability and super electromagnetic wave absorption performance. *Carbon* 135, 1–11. doi:10.1016/j.carbon.2018.04.026

Wang, Z., Xiao, P., and He, N. (2006). Synthesis and characteristics of carbon encapsulated magnetic nanoparticles produced by a hydrothermal reaction. *Carbon* 44, 3277–3284. doi:10.1016/j.carbon.2006.06.026

Wu, A., Yang, X., and Yang, H. (2012). Magnetic properties of carbon coated Fe, Co and Ni nanoparticles. *J. Alloys Compd.* 513, 193–201. doi:10.1016/j.jallcom.2011.10.018

Wu, X., Zhang, H., Huang, K.-J., and Chen, Z. (2020). Stabilizing metallic iron nanoparticles by conformal graphitic carbon coating for high-rate anode in Ni-Fe batteries. *Nano Lett.* 20, 1700–1706. doi:10.1021/acs.nanolett.9b04867

Xie, K., Jia, Q., Zhang, X., Fu, L., and Zhao, G. (2018). Electronic and magnetic properties of stone–wales defected graphene decorated with the half-metallocene of M (M = Fe, Co, Ni): A first principle study. *Nanomater. (Basel).* 8, 552. doi:10.3390/nano8070552

Yan, Y., Du, J. S., Gilroy, K. D., Yang, D., Xia, Y., and Zhang, H. (2017). Intermetallic nanocrystals: Syntheses and catalytic applications. *Adv. Mat.* 31, 1806746. doi:10.1002/adma.201806746

Yao, Y., Izumi, R., Tsuda, T., Aso, K., Oshima, Y., and Kuwabata, S. (2020). One-pot synthesis of PtNi alloy nanoparticle-supported multiwalled carbon nanotubes in an ionic liquid using a staircase heating process. *Acs Omega* 5, 25687–25694. doi:10.1021/acsomega.0c02951

Zhan, M., Pan, G., Wang, Y., Kuang, T., and Zhou, F. (2017). Ultrafast carbon nanotube growth by microwave irradiation. *Diam. Relat. Mater.* 77, 65–71. doi:10.1016/j.diamond.2017.06.001

Zhang, J., Tu, R., and Goto, T. (2011). Preparation of carbon nanotube by rotary CVD on Ni nano-particle precipitated cBN using nickelocene as a precursor. *Mat. Lett.* 65, 367–370. doi:10.1016/j.matlet.2010.09.074

Zhong, B., Mateu-Roldan, A., Fanarraga, M. L., Han, W., Munoz-Guerra, D., Gonzalez, J., et al. (2022). Graphene-encapsulated magnetic nanoparticles for safe and steady delivery of ferulic acid in diabetic mice. *Chem. Eng. J.* 435, 134466. doi:10.1016/j.cej.2021.134466

Zhou, J., Song, H., Chen, X., Zhi, L., Yang, S., Huo, J., et al. (2009). Carbon-encapsulated metal oxide hollow nanoparticles and metal oxide hollow nanoparticles: A general synthesis strategy and its application to lithium-ion batteries. *Chem. Mat.* 21, 2935–2940. doi:10.1021/cm9006266